Localization of the vibrational states of binary disordered linear chains*

R. D. Painter†
Naval Weapons Center,‡ China Lake, California 93555
and Department of Physics, Michigan State University, East Lansing, Michigan 48824

W. M. Hartmann
Department of Physics, Michigan State University, East Lansing, Michigan 48824

(Received 15 January 1974; revised manuscript received 2 September 1975)

We present the results of computer experiments to determine the localization of the eigenstates of a harmonic disordered linear chain with equal nearest-neighbor force constants and differing mass ratios, concentrations, and degrees of short-range order among two constituent atoms. We examine two measures of localization, the spatial extent of the modes and the decay length of the modes away from the region of appreciable strength. Experimentally, the two measures are found to agree at low frequencies but to behave oppositely at peaks of the impurity band. A one-particle Green's-function theory for the decay parameter is developed and is in good agreement with the experimental decay length in disordered chains. The same theory is applied to the decay of forced vibrations outside the bands of perfectly ordered chains.

I. INTRODUCTION

This paper is the third of a series of papers on the vibrations of a disordered harmonic linear chain. In the first paper,[1] we discussed the vibrational density of states of a chain with equal nearest-neighbor force constants and arbitrary concentrations of two kinds of atoms with different masses. In particular, we considered the effect of short-range order on the vibrational spectrum. By introducing the short-range order in terms of first- and second-order Markov processes, we found a technique for the computer generation of chains for numerical experiments In the second paper,[2] we presented cluster-theoretical calculations of the spectrum, which were compared with the spectra determined by the computer experiments. A self-consistent cluster method, analogous to the coherent-potential approximation, was found to be quite successful except for high degrees of short-range order. In this paper we consider the localization of the vibrational eigenstates of linear chains, similar to those of Refs. 1 and 2.

Our model is the same as that of Refs. 1 and 2. The equation of motion for the displacement u_l of the atom at site l is

$$\sum_{l'=1}^{N} (m_l \omega^2 \delta_{l,l'} - \phi_{l,l'}) u_{l'} = 0, \tag{1}$$

where the force-constant matrix $\underline{\phi}$ is translationally invariant,

$$\phi_{l,l'} = \gamma(2\delta_{l,l'} - \delta_{l,l'-1} - \delta_{l,l'+1}). \tag{2}$$

The atomic mass m_l may take on one of two values: m_h for host atoms, concentration $1-c$, and m_d for defect atoms, concentration c. By convention the defect atoms are always the lighter atoms so that $\mu \equiv m_h/m_d$ is greater than 1. Furthermore, we choose frequency units so that $\gamma/m_d = 1$.

Substantial work on the localization of eigenstates in disordered one-dimensional systems has been reported. Mott and Twose[3] conjectured, and Borland,[4] proved that all one-electron eigenstates of the disordered chain are localized. This proof is valid for eigenstates of arbitrarily large energy for an infinite chain with a finite fraction of disorder, and therefore applies to the exact solutions of a Schrödinger equation. Demonstration of localization in the lattice-dynamics problem does not require such a dramatic result. The lattice-dynamics problem is more akin to the one-band Anderson model,[5] where a one-electron site representation of the Hamiltonian has disordered diagonal elements and, usually, translationally invariant off-diagonal elements. Proofs of the localization of all the eigenstates of equation of motion (1) with only nearest-neighbor interactions have been given by Economou and Cohen[6] and by Dean[7] for glasslike chains with disordered force constants.

The localization theorems apply to infinite chains with a finite ($c > 0$) concentration of defects. The defect scattering strength, however, may be arbitrarily small. Important as these theorems are, they do not completely answer all questions about localization in one-dimensional systems. Though the states of an infinite system may be localized, one cannot say that all the states of a finite system of N sites are localized in the limit $N \to \infty$. This appears to be the basis of the counterargument of Taylor.[8] Moreover, as Halperin[9] has noted, the theorems are not sufficient to ensure the vanishing of transport coefficients. Most importantly, from our viewpoint, the localization theorems do not predict the length of the region of localization, nor do they apply to the eigenstates of *finite* disordered chains. Therefore, localization in one dimension

is still an interesting problem.

Several attempts have been made to find the fraction of nonlocalized vibrational states in finite one-dimensional harmonic random systems. Matsuda and Ishii[10] found that for mass-disordered chains the number of nonlocalized modes is

$$n = (4/\pi)\sqrt{N}\,\langle m\rangle/[\langle(m-\langle m\rangle)^2\rangle]^{1/2}, \tag{3}$$

where $\langle m\rangle$ is the average mass, $\equiv c m_d + (1-c)m_h$. Matsuda and Ishii allow that this formula is valid only to an order of magnitude since "nonlocalized" is not precisely defined. Visscher[11] made numerical studies of thermal energy transport in chains of 1000 atoms. He arbitrarily defined the eigenfrequency above which all states are localized as the eigenfrequency above which the sum of the remaining modes gives a contribution to the thermal conductivity of only 10%. Visscher obtained an empirical formula for the demarcation mode number of

$$n_c = 5.5(N)^{1/2} \tag{4}$$

for a random system with $\mu = 2$.

In Secs. II and III of this paper we discuss the measurement of localization by computer experiments on one-dimensional chains. For two chains of 1000 atoms we have calculated all the eigenvectors. Most of the eigenvectors have considerable detailed structure which is difficult to discuss in general terms. Therefore, we shall discuss the eigenstates in terms of a model mode shown in Fig. 1. This model mode contains the most important localization parameters. Parameter L' is the length over which the eigenstate has appreciable strength (approximately $|u_l|^2 \geq N^{-1}$). Parameter Λ is the exponential decay length away from the region of appreciable strength.

We now argue that the parameter

$$L \equiv \left[\sum_l u_l^4 \Big/ \left(\sum_l u_l^2\right)^2\right]^{-1} \tag{5}$$

is a good measure of the length L', expressed as number of sites. For our model mode of Fig. 1,

$$L = [L_f + \coth(1/\Lambda)]^2/[L_f + \coth(2/\Lambda)]. \tag{6}$$

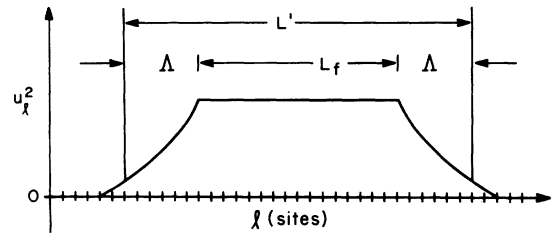

FIG. 1. Squared displacements u_l^2 for a model vibrational mode of a disordered chain with exponential decay Λ and spatial extent L'.

In the limit $\Lambda = 0$ we have $L = L_f + 1 = L' + 1$. Alternatively, if $\Lambda \geq 7$ sites, then

$$L \approx (L_f + \Lambda)^2/(L_f + \tfrac{1}{2}\Lambda) \tag{7}$$

and, therefore,

$$(L_f + \Lambda) < L \leq (L_f + 2\Lambda) \equiv L'. \tag{8}$$

The equality holds for $L_f = 0$.

The quantity L^{-1} is similar to a localization parameter discussed by Thouless[12] for an electron with wave function ψ in an infinite system

$$\int |\psi(r)|^4 d\Omega \Big/ \left(\int |\psi(r)|^2 d\Omega\right)^2, \tag{9}$$

where $d\Omega$ is a volume element appropriate to the system. The decay length Λ is similar to the decay length calculated by Bush[13] for one-electron wave functions of the Anderson Hamiltonian, and by Rubin[14] for lattice vibrations.

Another measure of the spatial extent of a mode, suggested by Thouless[12] and by Moore,[15] is the standard deviation σ of the mode, where

$$\sigma^2 = \sum_l u_l^2 (l - \bar{l})^2, \tag{10}$$

where

$$\bar{l} = \sum_l l u_l^2. \tag{11}$$

Moore defines the quantity $\mathfrak{L} = \sigma/\sigma_p$, where σ_p is the standard deviation for a perfect chain, $\sigma_p = N(12)^{-1/2}$ for both periodic and fixed boundary conditions. In order to compare the quantity $\mathfrak{L}$ with our measure L we calculate $N\mathfrak{L}$ for the model mode of Fig. 1. The final expression is rather cumbersome but it has several interesting limits,

$$\lim_{\Lambda \to 0} (N\mathfrak{L}) = [L_f(L_f - 1)]^{1/2}. \tag{12}$$

For $\Lambda \gg 1$ and $\Lambda \gg L_f$

$$N\mathfrak{L} = \Lambda\sqrt{6}. \tag{13}$$

In the former limit both the standard deviation and our measure L are the same except for L_f of order 1. For the second limit we can see that the standard deviation gives somewhat greater weight to the exponential tails than does our measure L. So long as the vibrational states have the simple form of Fig. 1 we would expect both measures of spatial extent to give approximately equal results. However, if a mode is localized in more than one region of the chain, then the two measures may differ appreciably. We observe that such modes with several well separated peaks do occur in our computer experiments.

II. AVERAGE DECAY LENGTH $\langle\Lambda\rangle$

One can calculate the displacements u_l from the equation of motion Eq. (1) in the form

$$u_{l+1} = [2 - (m_l/\gamma)\,\omega^2]\,u_l - u_{l-1}, \tag{14}$$

with fixed initial boundary conditions

$$u_0 = 0, \quad \text{and} \quad u_1 = 1. \tag{15}$$

As Dean[7] showed the u_l's will, on the average, increase exponentially as l increases. We therefore write

$$u_l \propto \exp[l/\Lambda(\omega^2)]\,. \tag{16}$$

A characteristic (decay) length Λ can be determined for the sequence of u_l's for any chain (determined by the set $\{m_l\}$ for arbitrary ω^2. Casher and Lebowitz[16] have shown that the spectrum of a infinite chain is not continuous on any interval. However we presume that for an infinite or semi-infinite chain an arbitrary value of ω^2 within the region of allowed frequencies is arbitrarily close to an eigenvalue, except for the insignificant number of special frequencies discussed in Ref. 1. Therefore, we presume that the configuration average value $\langle\Lambda(\omega^2)\rangle$, determined by averaging Λ's over a number of computations of the sequence of displacements, is equal to the average decay length of eigenstates of a semi-infinite chain.

We also wish to assume that the decay lengths determined by the sequence of u_l's are representative of decay lengths in long but finite chains. These assumptions have been discussed by other authors notably by Roberts and Makinson,[17] by Matsuda and Ishii,[10] and by Visscher,[11] and are further discussed in Sec. IV of this paper.

We calculate a configuration-averaged decay length by the following procedure. We start collecting data after some u_l satisfies $|u_l(\omega^2)| > e^4$. We then store the number of sites n we must pass before $|u_{l+n}(\omega^2)| > e^5$. We collect 30 values of n for a given computer-generated chain, i.e., u_l's vary from e^4 to e^{35}. The number of sites for an e increase in u_l is $\Lambda(\omega^2)$. We then find the mean and probable error of $\Lambda(\omega^2)$. We repeat this Monte Carlo experiment for 10 chains for each ω^2, finding 10 means and probable errors. We finally combine the results using a weighted mean and probable error. We find that the probable error associated with $\langle\Lambda(\omega^2)\rangle$ is usually less than 5% and the variability between chains is of the order of 10%.

Figure 2 shows $\langle\Lambda(\omega^2)\rangle$ vs ω^2 for binary random chains with $c = 0.5$ and mass ratios of $\mu = 1.5$, 2, and 3. In each case the frequency scale is such that $\gamma/m_d = 1$ or $\omega^2_{\max} = 4$. Therefore, the perfect heavy chain spectra would have maximum allowable frequencies of $\frac{8}{3}$, 2, and $\frac{4}{3}$, respectively. Some facts are immediately apparent. (i) In all cases the decay length tends to infinity as ω^2 tends to zero. (ii) The variation in the data from a definite functional relationship is small. (iii) The

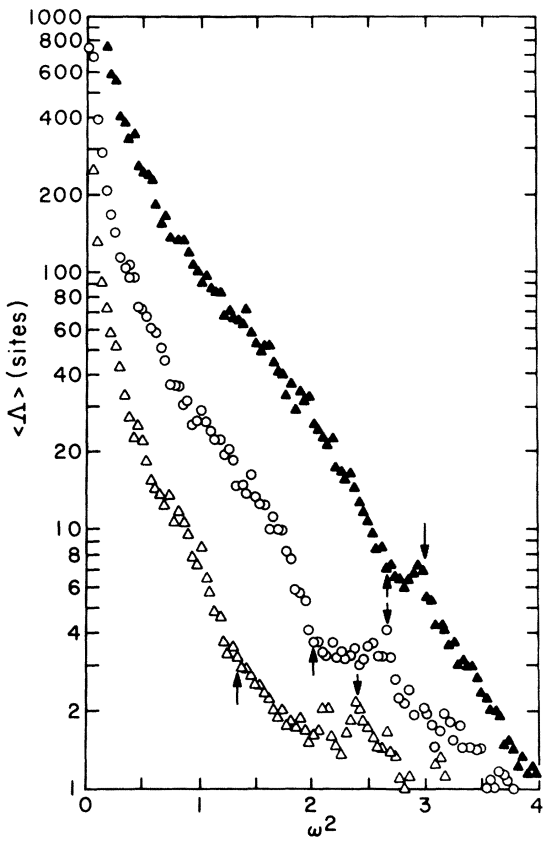

FIG. 2. Configuration averaged decay length for eigenstates of a random semi-infinite chain with 50% defects. ▲▲▲, $\mu = 1.5$; ooo, $\mu = 2$; ΔΔΔ, $\mu = 3.0$. The upward arrows indicate the top of the host band for each case. The downward arrows indicate the single-defect local-mode frequency.

data show an almost uniform decrease in decay length with increasing frequency. (iv) Increasing mass ratio decreases decay length at a given ω^2. Other trends are not as apparent. (i) An increase in mass ratio increases localization in both host and impurity bands. This can be seen by identifying an equivalent point in each case, e.g., the host band edge indicated by an upward arrow. (ii) Near the host band edge a marked drop in decay length is observed. (iii) The decay length is not monatomically decreasing with increasing ω^2. The $\mu = 1.5$ curve shows a peak at $\omega^2 = 2.94$. The $\mu = 2$ curve shows a peak at 2.66 and other peaks more clearly seen in Fig. 10. The $\mu = 3$ curve has a peak at 2.38, among others. Other plots, not shown here, for $\mu = 4$ and $\mu = 8$, have peaks, respectively, at $\omega^2 = 2.30$ and at 2.06. The frequencies of these peaks correspond well with the isolated-light-defect impurity frequency in each case. These local mode frequencies are $\omega^2 = 3$, $2\frac{2}{3}$, $2\frac{2}{5}$, $2\frac{2}{7}$, and $2\frac{2}{15}$ for mass ratios of $\mu = 1.5$, 2, 3, 4, and 8, respec-

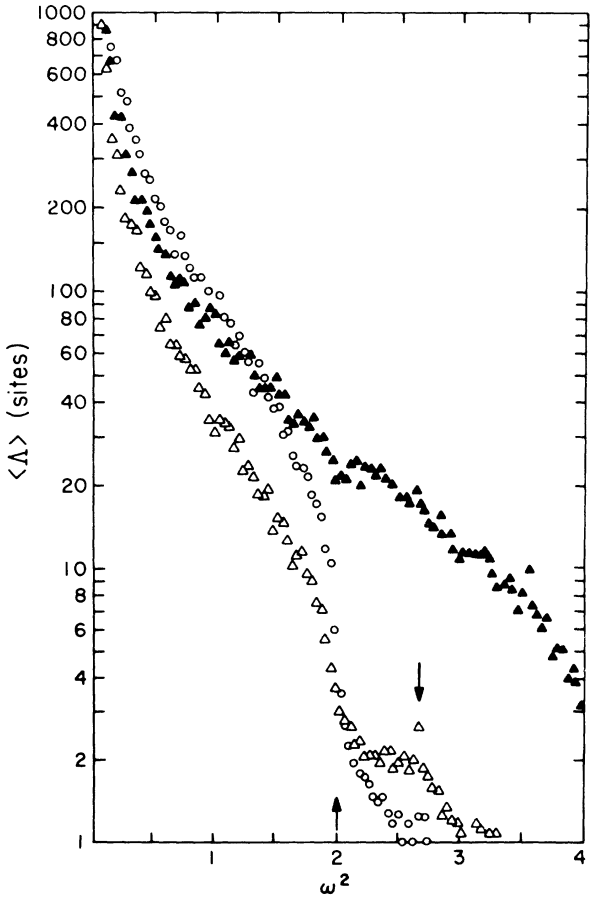

FIG. 3. Configuration averaged decay length for eigenstates of a random semi-infinite chain with $\mu = 2$ and various concentrations of defects: ○, $c = 0.1$; △, $c = 0.3$; ▲, $c = 0.9$. The host band edge is indicated by an upwards arrow. The local-mode frequency is indicated by a downwards arrow.

tively. We expect similar but smaller peaks at all the characteristic frequencies of isolated defect clusters in host mass chains. Such peaks can be seen in Fig. 10, which shows the results of a more detailed calculation of $\langle\Lambda\rangle$ for the case $\mu = 2$ and $c = 0.5$. For this graph we made a least-squares fit to the exponential increases of 10 different chains at each of 1000 points on the interval $0 < \omega^2 < 4$. The peak frequencies are independent of short-range order, which only changes the peak strengths. Comparing the peak frequencies with Table I of Ref. 2 we find peaks at all the impurity-band frequencies of *dd*, *ddd*, *dddd*, and *dhd* clusters.

Figure 3 shows $\langle\Lambda\rangle$ for random chains with $\mu = 2$ and concentrations of 0.1, 0.3, and 0.9. From these curves, and from similar curves for $c = 0.7$ (not shown) and for $c = 0.5$ (Fig. 2), we can identify some trends. (i) The decay length in the impurity band increases with increasing impurity concentration although not in a regular or uniform fashion. (ii) There is a marked decrease in the change in decay length at the host-band edge ($\omega^2 = 2$), varying from a change of an order of magnitude at $c = 0.1$ to a change of less than 10% for $c = 0.9$. (iii) The decay length in the host band is smallest for $c = 0.5$ and increases as $c \to 0$ or $c \to 1$. It is easy to offer a qualitative explanation of these trends. For $c < 0.5$ the chain is mostly made of heavy atoms with light impurities. As the concentration of light impurities increases the length of modes in the host band decreases owing to the increasing disorder. However, as the concentration of light impurities increases the modes of the impurity band can propagate more readily and become more delocalized. For $c > 0.5$ the chain is made of light atoms with heavy impurities. The majority band now extends to the maximum frequency $\omega^2 = 4$, and as $(1 - c)$ decreases the modes become more delocalized owing to decreasing disorder.

Figures 4 and 5 show $\langle\Lambda\rangle$ for $c = 0.5$, $\mu = 2$, and for first-order Markov transition probabilities of $p_{d,d} = 0.1$ and 0.3 for anticlustering of defects and 0.7 and 0.9 for clustering. Short-range order can radically modify the decay length at intermediate values of frequency. The chain with $c = 0.5$ and $p_{d,d} = 0.1$ resembles the ordered alternating chain ($c = 0.5$ and $p_{d,d} = 0$). As shown in Fig. 8 of Ref. 2 the spectrum for the anticlustering chain is a degraded perfectly alternating chain spectrum with a vestigial gap, $1 < \omega^2 < 2$, between an acoustic band and a vestigial optic band $2 \leq \omega^2 \leq 3$. Figure 4 shows that for the greater anticlustering the modes are more delocalized within the two bands. Precisely at the vestigial band edges, however, the two curves cross and the modes of the chain with the greater anticlustering are more localized in the "gap" region where propagation tends to be forbidden. Above the "edge" at $\omega^2 = 3$ the modes are so localized that they are insensitive to short-range order.

Figure 5 shows $\langle\Lambda\rangle$ for chains with two degrees of clustering. For $p_{d,d} = 0.9$ we have large clusters of like masses, and the structure of the host band is partly recovered over the random case, as shown in the density of states plot in Fig. 9 of Ref. 2. The decay length in the host band is greatly enhanced with a marked decrease outside this host band. Comparing Fig. 5 for $c = 0.5$ and $p_{d,d} = 0.9$ with Fig. 3 we see that the short-range order makes the decay length in the host band greater than that for the $c = 0.1$ random chain, an unexpected result. Near $\omega^2 = 0$, however, this is not the case. For the clustering chain it looks as if $\langle\Lambda(\omega^2)\rangle$ approaches 600 sites as ω^2 approaches zero and only the point at lowest ω^2 indicates that ac-

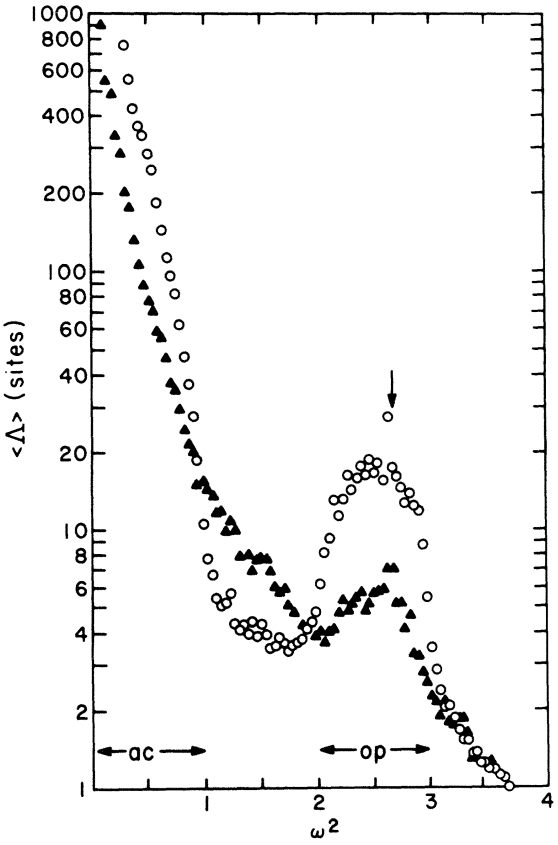

FIG. 4. Configuration averaged decay length for eigenstates of a semi-infinite chain with $c=0.5$ and $\mu=2$ for anticlustering short-range order, o, $p_{d,d}=0.1$; ▲, $p_{d,d}=0.3$. The regions of acoustic (ac) and optic (op) bands of the perfect alternating diatomic chain are shown.

tually $\Lambda(\omega^2)\to\infty$ as $\omega^2\to 0$. The curve with $p_{d,d}=0.7$ shows similar behavior, through the delocalization of the host band is less pronounced.

III. SPATIAL EXTENT (L)

To calculate our measure L of the spatial extent of an eigenstate we need to solve the equation of motion (1) for $u_l(\omega^2)$. These eigenvectors generally depend on the boundary conditions, an effect which we now consider by examining perfectly ordered systems. For periodic boundary conditions the normalized eigenvectors are $u_l \sim N^{-1/2} \times e^{ikl}$ and, therefore, $L=N$ for an ordered chain of N atoms. However, our computer experiments require fixed boundary conditions, $u_0=u_{N+1}=0$. Therefore, the normalized eigenvectors of a monatomic chain are

$$u_l=\left(\frac{2}{N+1}\right)^{1/2}\sin\left(\frac{\pi rl}{N+1}\right)\quad (r=1,2,\ldots,N). \tag{17}$$

Summing $\sin^4 kl$ over all sites we find $L=\frac{2}{3}(N+1)$. The situation is slightly different for a perfectly ordered alternating diatomic chain because L becomes a weak function of ω^2. The eigenstates of this chain occur in an acoustic band, $0\le\omega^2\le 2/\mu$, and an optic band $2\le\omega^2\le 2(1+\mu^{-1})$. We may easily calculate L at the four band edges because the motions of heavy and light atoms are simply related at these frequencies. The results are shown in Table I. Our numerical methods applied to an alternating chain of 100 free atoms confirm the values of L at special frequencies and show that L varies smoothly between these extreme values at the band edges as shown in Fig. 7.

The computation of the eigenvectors of a long disordered chain has previously been a stumbling block which has inhibited progress in the study of these chains.[16] We have discovered that the method of inverse reiteration is a satisfactory solution to this computational problem.[17] It is satisfactory in the sense that with it we are able to solve for the

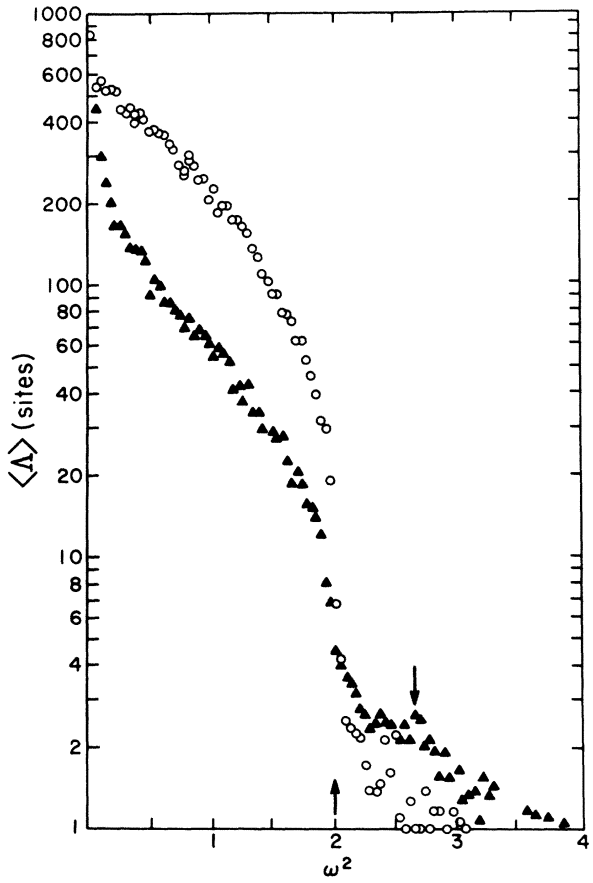

FIG. 5. Configuration averaged decay length for eigenstates of a semi-infinite chain with $c=0.5$ and $\mu=2$ for clustering short-range order: o, $p_{d,d}=0.9$; ▲, $p_{d,d}=0.7$. The host band edge is shown by the upward arrow. The local-mode frequency is shown by a downwards arrow.

TABLE I. Spatial extent parameter L at band edges for a perfectly alternating diatomic chain with mass ratio μ. The boundary atoms of the chain are fixed and N atoms between the boundaries are free to move.

ω^2	Mode	$L(\omega^2)$
0	$k=0$, acoustic	$\frac{2}{3}(N+1)$
$2/\mu$	ZB,[a] acoustic	$\frac{1}{3}(N+1)$
2	ZB, optic	$\frac{1}{3}(N+1)$
$2(1+\mu^{-1})$	$k=0$, optic	$[\frac{1}{3}(N+1)](\mu^2+1)^2/(\mu^4+1)$

[a]ZB, zone boundary.

eigenvectors of chains which are long enough to provide unambiguous indications of the behavior of eigenstates of an infinite chain. However, the procedure is not inexpensive. A convincing computation of L for $\mu=2$ requires a chain of ≈ 1000 atoms. The method of inverse reiteration requires 45-min CPU (central processing unit) on the Univac 1108 to solve for all the eigenvectors of the 1000-atom chain. Fortunately, the method allows the computation of single eigenvectors enabling a sampling of the band if desired. Once an eigenvector is calculated it is a simple matter to find L.

Figure 6 shows the localization plots for two different random 100-atom chains with $c=0.5$ and $\mu=2$. Since the chains are generated by a random-number generator there are different stochastic relationships between atoms in the two chains. Clearly $L(\omega^2)$ does not follow a definite functional relationship with ω^2. The spread in values for a single chain as well as the differences between the two chains might seem to make the data meaningless. This, however, is not the case. Because a 100-atom chain does not contain a representative set of eigenstates the data are not contradictory but complementary. We might add the results of many runs on 100-atom chains to get an improved data set. We feel that to average the results over some frequency interval as done by Moore[14] in his calculations of the standard deviation in glasslike chains is counterproductive. The spread in values of L at any given ω^2 clearly includes information about the variety of modes with appreciable strength at that frequency. Because of the fixed boundary conditions the values of L are not greater than $\frac{2}{3}N$. In order to estimate the fraction of the entire chain length included in a mode at frequency ω the calculated values of $L(\omega^2)$ may be divided by the values for the perfectly ordered chains shown in the figures. To help assess the validity of our results for L we can use the parameter $\langle\Lambda\rangle$ previously calculated for semi-infinite chains. Certainly the values of $L(\omega^2)$ for a 100-atom chain are not reliable for values of ω^2 where $\langle\Lambda\rangle > 50$ sites. From Fig. 2 with $\mu=2$ we can expect that our values of L would be good for $\omega^2 \geq 1.0$ where the exponential decay length is less than 30 sites, and very good for $\omega^2 \geq 2$, where $\langle\Lambda(\omega^2)\rangle < 5$ sites. The values of L below $\omega^2=0.5$ are almost certainly affected by the chain length, which means that these data do not have the generality which we ascribe to the other data. The eigenvectors in this region are extended over the whole 100-atom chain.

Figure 7 shows L for 100-atom chains with anticlustering ($p_{d,d}=0.1$) and clustering ($p_{d,d}=0.9$) short-range order. For the former case Fig. 4 suggests that L is chain-length limited for $\omega^2 \leq 0.9$. For the clustering case L should be severely chain-length limited for $\omega^2 \leq 1.9$, and not representative of the values of longer chains. With clustering of like atoms a short chain gives especially poor statistical relationships. Looking at the composition of this particular chain we can easily identify the modes in the region $2 < \omega^2 < 4$, all of which show a rapid decrease away from the region of appreciable displacements [$\langle\Lambda(\omega^2)\rangle \approx 1$]. The chain has the following structure:

$$11d\text{-}9h\text{-}6d\text{-}7h\text{-}21d\text{-}3h\text{-}3d\text{-}6h\text{-}$$

$$8d\text{-}3h\text{-}1d\text{-}10h\text{-}10d\text{-}1h\text{-}1d,$$

with $c=0.61$. The isolated impurity at site 78 produces the states at $\omega^2=2.667$, with $L=1.55$. The defect cluster of three atoms gives $L=3$ at eigenfrequencies $\omega^2=3.52$ and 2.414. Other points arise from the other clusters as noted in paren-

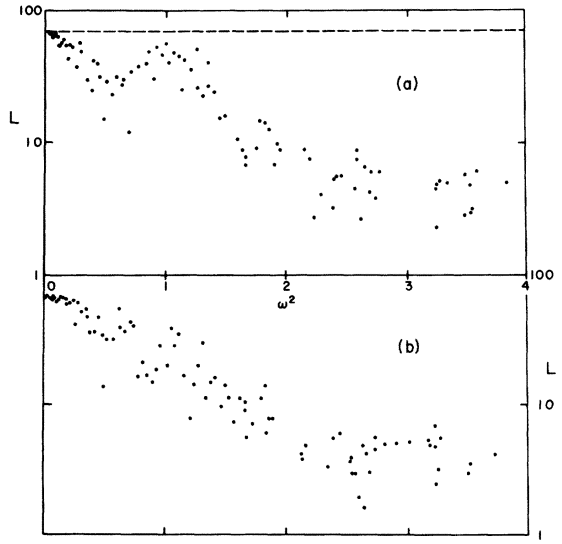

FIG. 6. Spatial extent of the eigenstates of two specific 100-atom random chains (a) and (b) with $c=0.5$ and $\mu=2$. The dashed line at $\frac{2}{3}(N+1)$ shows the extent of modes in a perfect monatomic 100-atom chain with fixed boundaries.

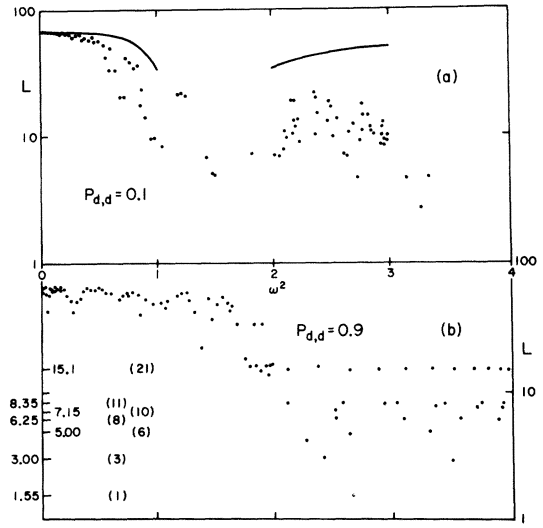

FIG. 7. Spatial extent of the eigenstates of specific 100-atom chains with $c=0.5$, $\mu=2$ and a large amount of short-range order. (a) anticlustering $p_{d,d}=0.1$; (b) clustering $p_{d,d}=0.9$. In (a) the solid line shows the extent of modes in a perfect alternating diatomic chain with fixed boundary conditions giving the band-edge limits of Table I. In (b) the strings of points with constant L are identified with the clusters of (i) defects discussed in the text.

theses on the figure.

Figure 8 shows L vs ω^2 for a random 1000-atom chain with $c=0.5$, $\mu=2$. The maximum $L(\omega^2)$ is 667.3, equal to that for the perfect monatomic chain. Figure 2 indicates that some values of L could be chain-length limited for $\omega^2<0.4$, but other values are probably valid. To get accurate values of L for the region $0.02<\omega^2\leq 0.4$ would require approximately $N=10\,000$. A negligibly small number of higher-frequency modes can be chain-length limited because they happen to have their appreciable displacements near one end of the chain. It is instructive to compare $L(\omega^2)$ in Fig. 8 with the density of states $D(\omega^2)$ in Fig. 5 of Ref. 2 for a 100 000-atom chain. The density of states of the 1000-atom chain, appropriate to Fig. 8, differs only in details as follows: The host band is considerably more ragged, exhibiting 50% fluctuations for $0.5<\omega^2\leq 2$. Some of the zeros in the impurity band are almost twice as wide as those in the case $N=100\,000$. However, the 11 major peaks in the impurity band are the same for both chain lengths, and for qualitative comparison all the above differences are unimportant. Since a dot in Fig. 8 represents an eigenstate, the zeros in the frequency spectrum at $\omega^2=2, 3, 3.414$, and 3.618 are clearly visible. The

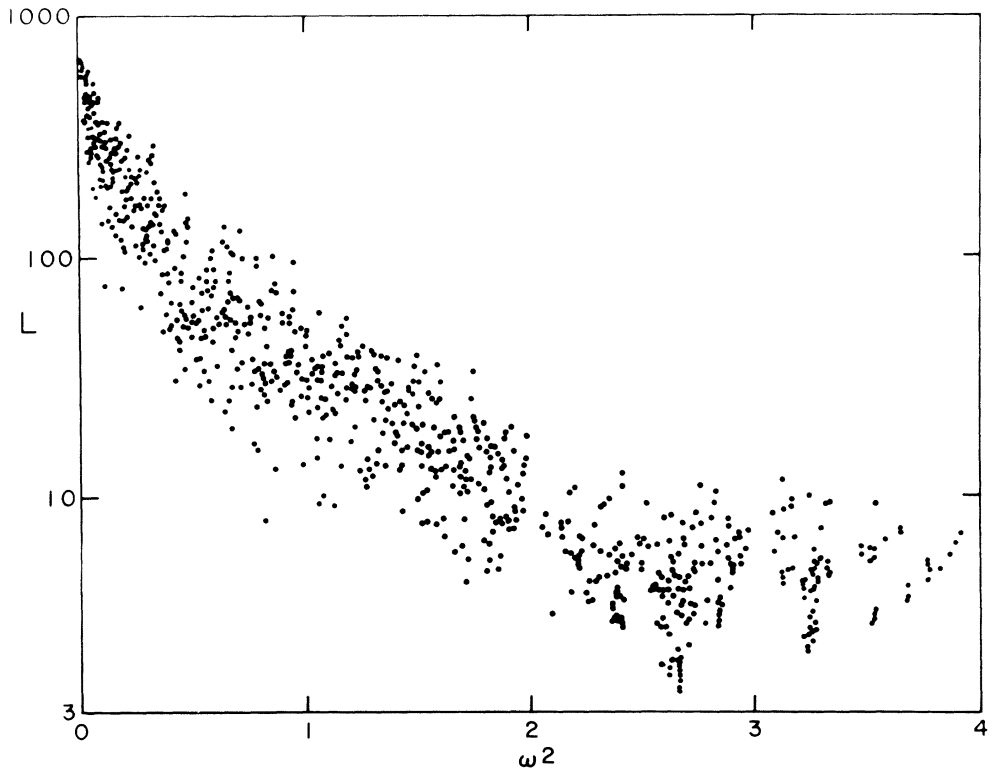

FIG. 8. Spatial extent of the eigenstates of a specific 1000-atom random chain with $c=0.5$ and $\mu=2$.

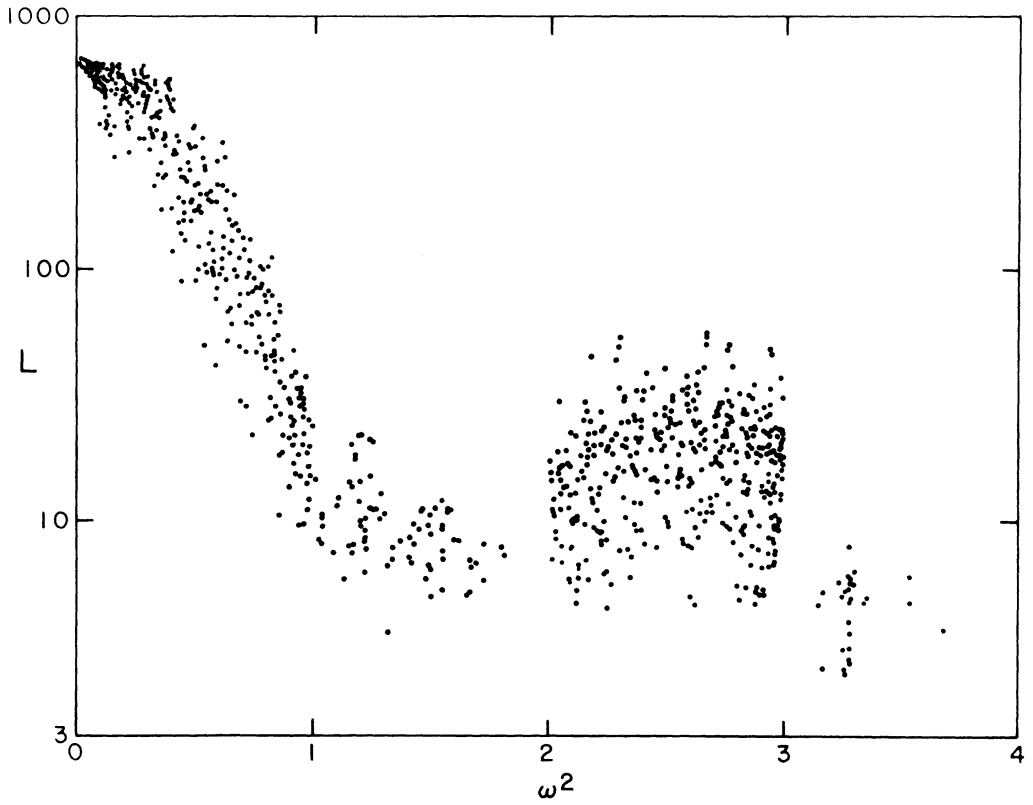

FIG. 9. Spatial extent of the eigenstates of a specific 1000-atom chain with $c = 0.5$ and $\mu = 2$ and anticlustering short-range order, $p_{d,d} = 0.1$.

clustering of points around defect cluster frequencies is also clearly seen. By the arguments given in the discussion of Fig. 7 we can explain the various series of points with $L(\omega^2)$ constant in the impurity band.

Figure 9 plots L vs ω^2 for a 1000-atom chain $\mu = 2$, $c = 0.5$, and $p_{d,d} = 0.1$. It may be compared with the density of states in Fig. 8 of Ref. 2. Comparing with the plot of $\langle\Lambda\rangle$ in Fig. 4(a) we note that some values of L may be chain-length limited for $\omega^2 < 0.5$. Since some of the modes in the vestigial optic band, $2 < \omega^2 \leq 3$, are 100 sites long the calculations for a 100-atom chain in Fig. 7(a) cannot completely describe the localization in this band.

We now compare the plots of L in Fig. 8 and Fig. 9 with the appropriate plots of $\langle\Lambda\rangle$ in Fig. 10. Several significant facts are apparent as follows. In part of the host band, $0 < \omega^2 < 1.54$, a line drawn through the center of gravity of the points $L(\omega^2)$ agrees with $\langle\Lambda(\omega^2)\rangle$ both in shape and in absolute values, a result which we had no reason to expect. In particular, in the region $0.5 < \omega^2 < 1$, both $\langle\Lambda\rangle$ and L have positive curvature for random chains [Figs. 8 and 10(a)], and both $\langle\Lambda\rangle$ and L have negative curvature for chains with anticlustering short-range order [Figs. 9 and 10(b)]. Comparing all four plots on Figs. 4 and 5 we can surmise that the negative curvature of $\langle\Lambda\rangle$ appears for both clustering and anticlustering chains when $p_{d,d}$ differs by $\approx \pm 0.3$ from its random value of 0.5. Towards the top of the host band $L(\omega^2)$ is rather flatter than $\langle\Lambda(\omega^2)\rangle$ but the two measures of localization still agree qualitatively. In the impurity band $\langle\Lambda\rangle$ continues to decrease with increasing ω, whereas the center of gravity of L seems to be approximately constant. Most interesting, the two measures of localization behave in opposite ways at the local mode frequency ($\omega^2 = 2.667$) and at the characteristic frequencies of other small clusters. (See Table I of Ref. 2.) Whereas the local mode has a *smaller spatial extent* (L) than do modes at nearby frequencies, the local mode *decays less rapidly* than do nearby modes. In Fig. 8 for L we believe that we can identify (*dd*) modes at $\omega^2 = 3.24$, (*ddd*) and (*dhd*) modes at $\omega^2 = 2.41$, (*dhd*) and (*dddd*) modes at $\omega^2 = 2.84$, and a (*ddd*) mode at 3.52. At these points $L(\omega^2)$ shows downward spikes. Figure 10(a) for $\langle\Lambda(\omega^2)\rangle$ shows a similar structure with upward

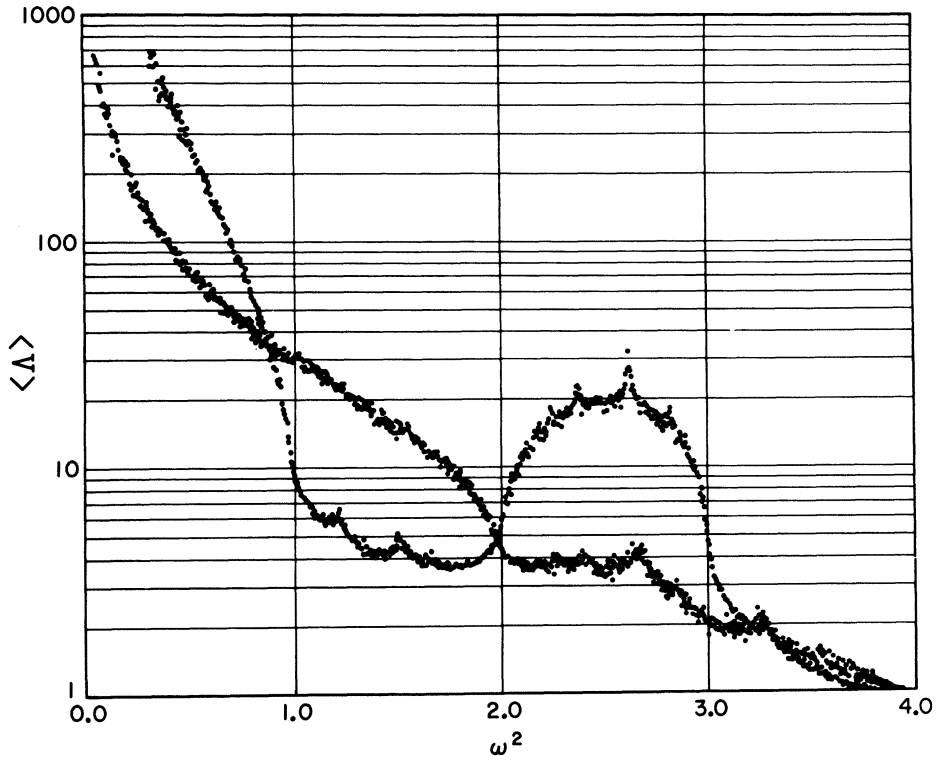

FIG. 10. A more detailed calculation of the configuration averaged exponential decay length for semi-infinite disordered chains with $c = 0.5$ and $\mu = 2$. Points (a) are for a random chain. Points (b) are for $p_{d,d} = 0.1$.

spikes.[18]

IV. THEORY AND DISCUSSION

In Secs. II and III we presented the results of computer experiments for two measures of localization of the eigenstates of a disordered chain with nearest-neighbor interactions. We calculated the average decay parameter $\langle\Lambda\rangle$ and the spatial extent L. There are several kinds of difficulties associated with the comparison of these two measures of localization. We have insisted that $\langle\Lambda\rangle$ be calculated for a semi-infinite chain so that any value of ω^2 is arbitrarily close to an eigenvalue except for special discrete points. Therefore, the sequences of displacements generated from the equation of motion are arbitrarily close to the beginning of eigenvectors of the semi-infinite chain. The assumption that the exponential rise of the sequence of displacements is equal to the decay length of eigenstates in a long but finite chain in the same region of frequency has been called the IF assumption.[10] Visscher[11] has found evidence in support of this assumption in his transport studies. Our test of the IF assumption is to compare Fig. 10(a) for the decay length of modes of an infinite chain with Fig. 11 for a finite chain. To create Fig. 11 we began with accurate eigenvalues and a complete set of eigenvectors for a specific 1000-atomic random chain. We found the actual decay lengths by a least-squares fit of an exponential to 711 eigenstates increasing over 5 powers of e.

The comparison indicates that for a determination of over-all features of the decay length, though perhaps not for exact results, our procedures are adequate. Not only does the IF assumption appear to hold satisfactorily but the finite accuracy of the iteration procedure of part II seems to lead to the correct exponential increase. The finite chain results of Fig. 11 confirm both the general behavior of $\langle\Lambda\rangle$ and the peaks in $\langle\Lambda\rangle$ at the mode frequencies of small clusters.

Recently the elements of a theory for Λ or $\langle\Lambda\rangle$ of such a chain have been established by Herbert and Jones[19] and further discussed by Thouless.[20] Also Papatriantafillou[21] has proposed an expression for the decay length in terms of the renormalized locator expansion of Economou and Cohen.[22] Very recently Sen[23] has shown that these two approaches lead to identical expressions for the decay length. The theories for the decay length relate it to a single-particle one-electron Green's function. In this section we increment theoretical progress on decay lengths by applying the Green's-

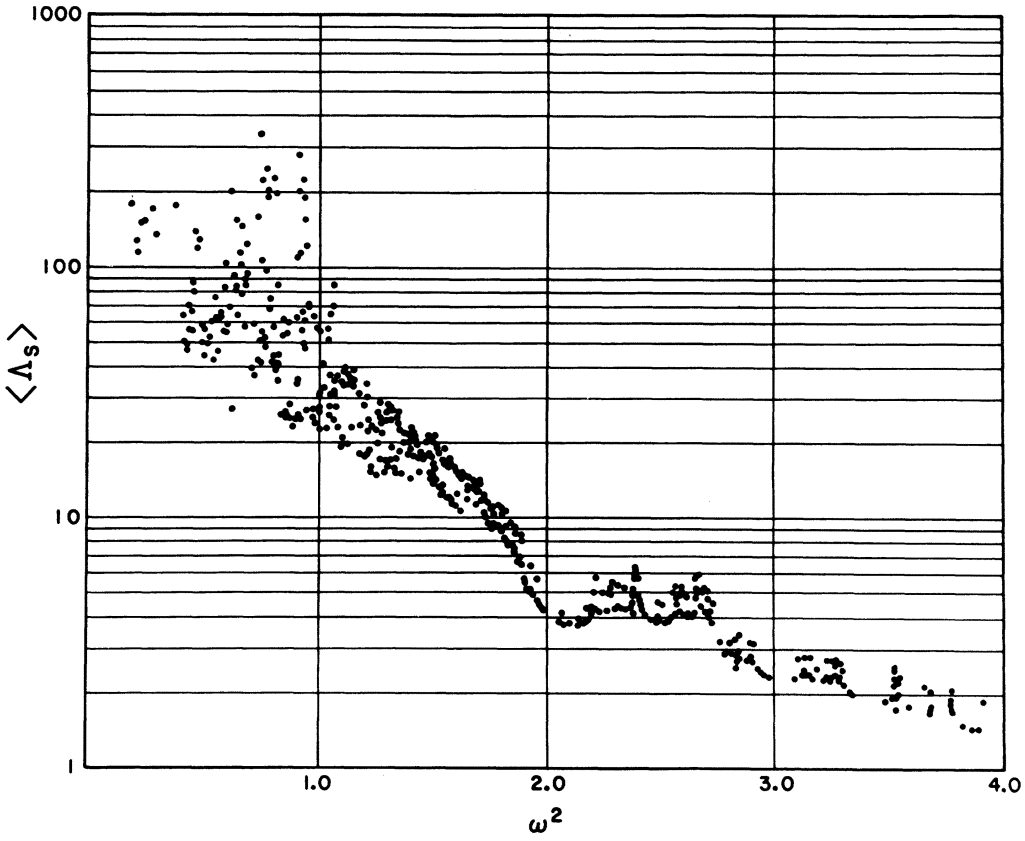

FIG. 11. Λ_s is the decay length for the eigenstates of a specific 1000-atom random chain (that of Fig. 8). Comparison with Fig. 10(a) tends to confirm the IF assumption and our numerical methods.

function ideas to lattice dynamics and the calculation of Λ.

By contrast there is no proper theory for L, which appears to require a two-particle Green's function for its description. There are theories for two-particle Green's functions in disordered systems within the context of the coherent-potential approximation.[24,25] However, a comparison of $\langle L(\omega^2)\rangle$ from a configuration-averaged theory with the results of our computer experiments on specific chains is likely to be disappointing because the experimental results exhibit considerable deviations from the mean.

On the other hand we shall find that $\Lambda(\omega^2)$ is simply related to the density of states. In the Appendix of Ref. 2 we showed that the density of states is sharply distributed about its configuration average and, thus, $\Lambda(\omega^2)$ is sharply distributed. We have tested the sharpness of the distribution of Λ by calculating $\Lambda(\omega^2)$ for a given finite chain of 1000 atoms with ω^2 equal to the eigenvalues of that particular chain. For $\omega^2 < 1$ the scatter in Λ is as great as that in L, but for $\omega^2 > 2$ the scatter in Λ is no greater than that in $\langle\Lambda\rangle$ shown in Fig. 10.

We therefore present a theory for Λ and the result for $\langle\Lambda\rangle$ follows immediately.[26]

The theory requires that the equation of motion for u_l be equivalent to a tridiagonal matrix. Therefore, we are restricted to a chain with nearest-neighbor interactions only. However, it is easy to incorporate force-constant changes and we shall add this generality by replacing the translationally invariant force-constant matrix of Eq. (2) with

$$\phi_{l,l'} = -\gamma_l \delta_{l,l'+1} - \gamma_{l+1}\delta_{l,l'-1} + (\gamma_l + \gamma_{l+1})\delta_{l,l'}. \tag{18}$$

We introduce the usual Green's operator

$$\hat{G} = (\hat{M}\omega^2 - \hat{\phi})^{-1}, \tag{19}$$

and a mass-reduced Green's operator

$$\hat{F} = \hat{M}^{1/2}\hat{G}\hat{M}^{1/2}. \tag{20}$$

In a local representation $\{|l\rangle\}$ the operator $\hat{M}^{1/2}$ is diagonal with $\sqrt{m_l}$ at site l. The Green's operator $\hat{F}$ is diagonalized by the eigenstates $\{|\alpha\rangle\}$ of the system,

$$\langle\alpha|\hat{F}|\beta\rangle = \delta_{\alpha,\beta}(\omega^2 - \omega_\alpha^2)^{-1}. \tag{21}$$

Therefore,

$$\langle l\,|\,\hat{G}\,|\,l'\rangle = (m_l m_{l'})^{-1/2} \sum_\alpha \frac{\langle l|\alpha\rangle\langle\alpha|l'\rangle}{\omega^2-\omega_\alpha^2}\,. \qquad (22)$$

From the equation of motion, Eq. (1), we find the local representation of eigenstate $|\beta\rangle$

$$\langle l\,|\beta\rangle = m_l^{1/2}\,u_l(\beta)\,, \qquad (23)$$

where $u_l(\beta)$ is the displacement of the atom at site l in the mode β. Therefore,

$$u_l(\beta)\,u_{l'}^*(\beta) = \langle l\,|\,\hat{M}^{-1/2}\,|\beta\rangle\langle\beta\,|\,\hat{M}^{-1/2}\,|\,l'\rangle\,, \qquad (24)$$

which can be expressed as a residue of G.

In particular, for a chain with $1 \le l \le N$,

$$u_1(\beta)\,u_N^*(\beta) = \lim_{\omega^2\to\omega_\beta^2} (\omega^2-\omega_\beta^2)\langle 1\,|\,\hat{G}\,|\,N\rangle\,. \qquad (25)$$

The calculation of the $(1, N)$ element of the inverse from Eq. (19) is easy for a chain with nearest-neighbor interactions because the cofactor is the determinant of a lower triangular matrix. Therefore we find

$$|u_1(\beta)\,u_N(\beta)| = \Big(\prod_{l=1}^{N-1}|\gamma_l|\Big)\Big/\Big((\mathrm{Det}\hat{M})\prod_{\substack{\alpha=1\\(\alpha\neq\beta)}}^{N}|\omega_\beta^2-\omega_\alpha^2|\Big). \qquad (26)$$

We now make the exponential decay hypothesis

$$|u_1(\beta)\,u_N(\beta)| = \exp[-(N-1)/\Lambda_\beta]. \qquad (27)$$

Neglecting the difference between N and $N-1$ and unimportant boundary effects, and replacing the sum over eigenstates α with an integral over the density of states $D(\omega^2)$, we find

$$\Lambda^{-1}(\omega_\beta^2) = \int D(\omega^2)\ln|\omega_\beta^2-\omega^2|\,d\omega^2 - \langle\ln(\gamma/m)\rangle = \int D(y)\ln|y_\beta - y|\,dy, \qquad (28)$$

where $y \equiv \omega^2/\omega_G^2$. The normalizing frequency ω_G is calculated from the configuration average above:

$$\omega_G^{2N} = \prod_{l=1}^{N}\frac{\gamma_l}{m_l}\,, \qquad (29)$$

a geometric mean over the configurations of a local frequency. From Eq. (28) a theoretical decay length can be calculated. Another perspicuous form is obtained by differentiating

$$\frac{d\Lambda_\beta^{-1}}{d\omega_\beta^2} = \frac{1}{N}\sum_l \mathrm{Re}\,F_{ll}. \qquad (30)$$

For a configuration averaged decay length,

$$\frac{d\langle\Lambda(\omega^2)\rangle^{-1}}{d\omega^2} = \mathrm{Re}\,\langle F_{ll}(\omega^2)\rangle\,. \qquad (31)$$

The real part of the diagonal Green's function is zero within any band of any ordered chain, and the eigenstates of an ordered chain are delocalized ($\Lambda_\beta = \infty$) in the Borland sense. We may use these facts to study the decay length of forced vibrations of a perfect chain outside the bands of normal modes.

An ordered chain with a basis of n atoms will have n bands with bottom frequencies b_i and top frequencies t_i. Then in any gap, or above all bands,

$$\Lambda^{-1}(\omega) = \sum_{\alpha=1}^{n}\int_{t_i^2}^{\omega^2}\mathrm{Re}\,F_{00\alpha\alpha}^0(\omega'^2)\,d\omega'^2 \qquad (t_i < \omega < b_{i+1}). \qquad (32)$$

The sum over basis atoms α in the unit cell of the perfect chain replaces the configuration average of the disordered chain.

For a monatomic chain

$$\Lambda^{-1}(\omega) = 2\ln\{\omega/\omega_{\max} + [(\omega^2/\omega_{\max}^2)-1]^{1/2}\} \qquad (\omega > \omega_{\max}), \qquad (33)$$

shown as the solid line (a) on Fig. 12. This result can also be found by a direct calculation of

$$\Lambda^{-1}(\omega) = (1/N)\ln[G_{0N}(\omega^2)/G_{00}(\omega^2)]\,, \qquad (34)$$

which proves that outside the bands of a perfect chain the decay is exponential.

For an alternating diatomic chain with nearest-neighbor interactions we use the Green's functions of Sen and Hartmann[27] to find

$$\Lambda^{-1}(\omega) = \pm\ln\left(\frac{(|x^2 - xX_T|)^{1/2} \pm [|x-X_0|(x-X_A)]^{1/2}}{(X_0 X_A)^{1/2}}\right), \qquad (35)$$

where $x = \omega^2$, X_A and X_0 are acoustic and optic zone boundary frequencies squared, and the top of the optic band is $X_T = X_A + X_0$. The plus signs are used above the bands ($\omega^2 > X_T$) and the minus signs are used in the gap ($X_A < \omega^2 < X_0$). This result is plotted on Fig. 12 for Λ as a solid line (b). We notice that for both monatomic and diatomic perfect chains the decay length outside the bands tends to be shorter than that for modes of the same frequency in the disordered system. This result makes some sense because the perfect chains include no impurities to help propagate the forced vibration. However, there are logical difficulties in trying to establish a perfect chain Λ as a lower bound to Λ for a disordered system, because there is no way to identify a particular ordered chain as the proper ordered limit of a disordered chain. The correspondences implied by the figures of this paper are suggestive but have no rigorous basis.

In Fig. 12 we plot the theoretical decay lengths calculated from Eq. (28) using 200 point densities

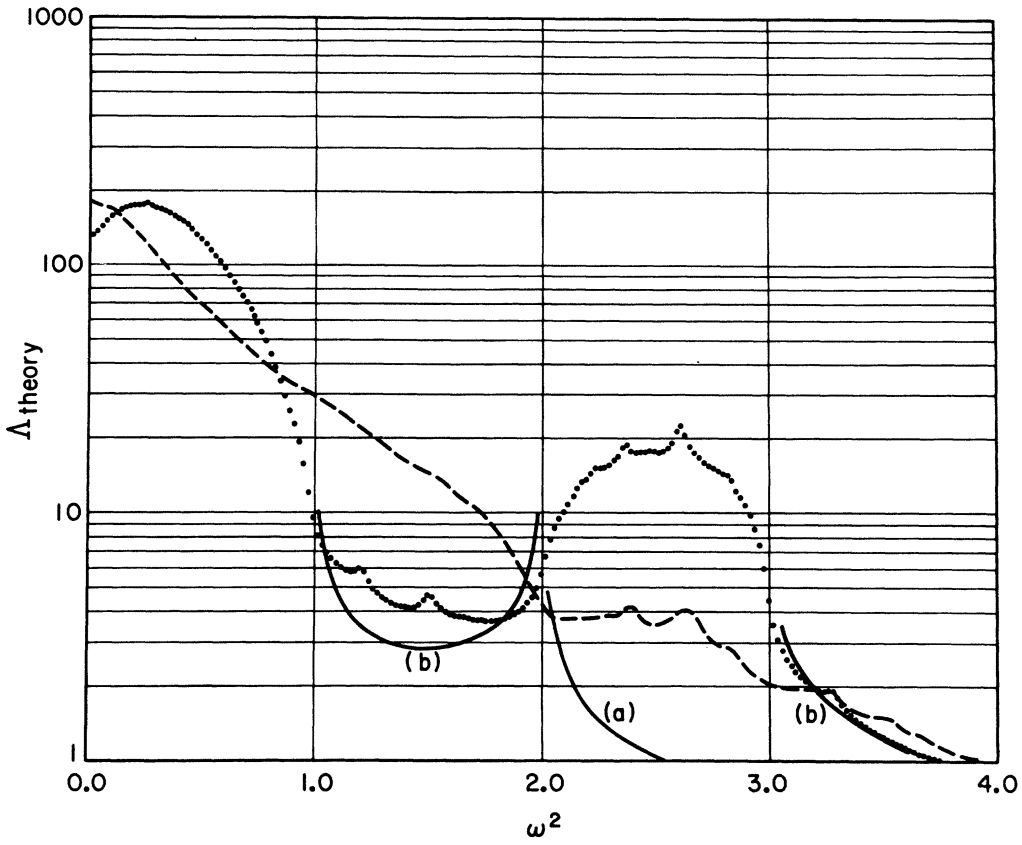

FIG. 12. Theoretical exponential decay length calculated from 200 point densities of states of disordered chains with $c=0.5$ and $\mu=2$. The dashed curve is for a random chain. The dotted curve is for $p_{dd}=0.1$. The solid curves show the theoretical decay lengths for perfect chains. Curve (a) is for a monatomic chain, $m_h=2$. Curve (b) is for the alternating binary chain.

of states for random and anticlustering chains of 100 000 atoms. The agreement with the experimental Λ in Fig. 10 is almost exact except for $\omega^2 < 0.7$. At these low frequencies Λ^{-1} is small due to cancellation within the integral, and our numerical integration is not sufficiently accurate for a proper calculation of Λ.

ACKNOWLEDGMENTS

We wish to thank Dr. R. L. Bush, Dr. P. N. Sen, and Dr. W. M. Visscher for helpful discussions.

*Work supported by the NSF Grant No. GH 34565.

†Paper includes excerpts from a thesis submitted in partial fulfillment of the requirements for the degree of Doctor of Philosophy at Michigan State University.

‡Present address.

[1]R. D. Painter and W. M. Hartmann, Phys. Rev. B 10, 2159 (1974).

[2]R. D. Painter and W. M. Hartmann, submitted to Phys. Rev. B (to be published).

[3]N. F. Mott and W. D. Twose, Adv. Phys. 10, 107 (1961).

[4]R. E. Borland, Proc. R. Soc. Lond. A 274, 529 (1963).

[5]P. W. Anderson, Phys. Rev. 109, 1492 (1958).

[6]E. N. Economou and M. H. Cohen, Phys. Rev. B 4, 396 (1971).

[7]P. Dean, Proc. Phys. Soc. Lond. 84, 727 (1964).

[8]P. L. Taylor, Phys. Lett. 18, 13 (1965).

[9]B. I. Halperin, Adv. Chem. Phys. 13, 123 (1967).

[10]H. Matsuda and K. Ishii, Prog. Theor. Phys. Suppl. 45, 56 (1970).

[11]W. M. Visscher, Prog. Theor. Phys. 46, 729 (1971).

[12]D. J. Thouless, J. Non-Cryst. Solids 8-9, 461 (1972).

[13]R. L. Bush, Phys. Rev. B 6, 1182 (1972).

[14]R. J. Rubin, J. Math Phys. 9, 2252 (1968); also R. J. Rubin and W. L. Greer, *ibid.* 12, 1686 (1971), and references therein.

[15]E. J. Moore, J. Phys. C 6, 1551 (1973).

[16]A. Casher and J. L. Lebowitz, J. Math. Phys. 12, 1701 (1971).

[17]A. P. Roberts and R. E. B. Makinson, Proc. Phys. Soc. Lond 79, 630 (1962).

[18]Note upon revision: There are many eigenvectors with L values less than $\langle\Lambda\rangle$ evaluated at the corresponding frequency. For such cases our model mode of Fig. 1 is a particularly inappropriate picture. The eigenstates for such modes exhibit sharp peaks separated by regions of smaller amplitude. The picture of E. N. Economou and C. Papatriantafillou [Phys. Rev. Lett. 32, 1130 (1974)] appears to apply to most of these cases. In a few other cases for $\omega^2 > 3.0$ the eigenvectors can be strongly localized in several different regions of the chain.

[19]D. C. Herbert and R. Jones, J. Phys. C 4, 1145 (1971).

[20]D. J. Thouless, J. Phys. C 5, 77 (1972).

[21]C. Papatriantafillou, Phys. Rev. B 7, 5386 (1973).

[22]E. N. Economou and M. H. Cohen, Phys. Rev. B 4, 396 (1971); 5, 2931 (1972).

[23]P. M. Sen, Solid State Commun. 13, 1693 (1973).

[24]B. Velicky, Phys. Rev. 184, 614 (1969).

[25]P. L. Leath, Phys. Rev. B 2, 3078 (1970).

[26]Phase theories have been applied to studies of Λ, by R. L. Agacy and R. E. Borland, Proc. Phys. Soc. Lond. 84, 1017 (1964); and by A. Bogan, Phys. Rev. B 8, 1656 (1973).

[27]P. N. Sen and W. M. Hartmann, Phys. Rev. B 9, 367 (1974).